Metals and Materials International (2021) 27:1769–1778
https://doi.org/10.1007/s12540-019-00553-3

Influence of SiAlON Ceramic Reinforcement on Ti6Al4V Alloy Matrix via Spark Plasma Sintering Technique

Oluwasegun Eso Falodun[1] · Samuel Ranti Oke[1,2] · Babatunde Abiodun Obadele[3] · Avwerosuoghene Moses Okoro[1] · Peter Apata Olubambi[1]

Received: 13 September 2019 / Accepted: 19 November 2019 / Published online: 28 November 2019

Abstract
The titanium-based composite was fabricated by strengthening Ti6Al4V alloy with addition of SiAlON ceramics utilizing spark plasma sintering technique. Ti6Al4V and SiAlON powders were mixed in a T2F Turbula mixer with different proportions (5, 10, 15 and 20 vol%) and the admixed powders were consolidated using spark plasma sintering to produce titanium matrix composites. The characterization of the sintered composites was performed using X-ray diffraction, optical microscopy and scanning electron microscopy. The influence of SiAlON additions on densification, microstructure, microhardness and fracture morphology were investigated on the sintered composites. The experimental results revealed that the densification of the sintered titanium matrix composites was in the range of 95%–98%, which decreased with an increase in SiAlON addition. However, an increase in microhardness values ranging from 363 to 574 $HV_{0.1}$ was achieved. The microstructure shows that the SiAlON ceramic particle was uniformly distributed within the titanium matrix composites which comprises of a mixture of lamellar colonies with β grain boundaries. The fracture features of all composites exhibit mixed fracture of both intergranular and transgranular fracture mechanism.

Keywords Powder metallurgy · Ti6Al4V · SiAlON · Reinforcement · Characterization

1 Introduction

Titanium and titanium alloys remain one of the significant class of materials that finds its application in various industries such as aerospace, automotive and medical fields. Because of outstanding properties, its possess such as weight reduction, high specific strength and corrosion resistance properties that meet the growing demand for saving energy consumption and cost [1, 2]. Despite the excellent physical and mechanical properties of titanium alloys, these materials is deprived of surface interaction in relative motion that limits their application for some engineering purposes [3, 4]. Thus, researchers are focusing more attention on enhancing the mechanical properties of titanium alloys through different strengthening mechanisms and modification in the previous technique [5–7]. Also, different researchers have strengthened titanium alloys with ceramic particles additives using spark plasma sintering technique and their influence on both the wear and mechanical properties of titanium alloys such as TiN [8], TiB_2 [9], ZrB_2 [10]. However, SiAlON ceramics also comprise an alternative class of materials that have numerous distinctive properties which include high strength, hardness, wear resistance, high melting temperature, high thermal conductivity and excellent thermal shock resistance [11–14].

Powder metallurgy (PM) increases as an attractive choice to withstand a strategic in avoiding the presence of undesirable phases in material and as well provide an economic strategy in developing small components with intricate shapes and great dimensional tolerance. There are different sintering techniques used in the production of titanium matrix composite which includes hot pressing, hot isostatic pressing, pressureless sintering, microwave sintering and spark plasma sintering. One of the developed sintering methods

✉ Oluwasegun Eso Falodun
segzy201@gmail.com

[1] Centre for Nanomechanics and Tribocorrosion, University of Johannesburg, Johannesburg, South Africa

[2] Department of Metallurgical and Materials Engineering, Federal University of Technology, Akure P.M.B. 704, Nigeria

[3] Department of Chemical, Material and Metallurgical Engineering, Botswana International University of Science and Technology, Palapye, Botswana

is spark plasma sintering (SPS) which has recently become common in use and has attracted significant attention for powder metallurgy due to certain characteristics of its heating mechanism [15] when compared with conventional sintering methods. The application of Joule heating, where direct current is passed through the raw powder and graphite die which produces spark discharge between the conductive particles strongly heat up and complete densification in a short period with a temperature lower the melting point of the raw powders. Also, in respect to rapid densification, SPS promotes the development of necking between particles and thus efficiently increases the sinterability of the particles with a higher density and limited grain growth [16, 17].

The interesting properties of SiAlON materials have made these materials useful for different superior applications [18]. The objective of this research was to produce spark plasma sintered Ti6Al4V alloy matrix with a varied amount of SiAlON ceramic ranging from 5 to 20 vol% and to investigate their influences on the densification mechanism, microstructural, phase transformation, density, hardness and fractography of the sintered composites.

2 Experimental Procedure

2.1 Materials Preparation

Ti6Al4V powder (APS 25 μm: Purity 99.9%) supplied by TLS-Technik, Germany and SiAlON powder (APS 45 μm: Purity 97%) supplied by Weartech Pty were used as the starting materials. Ti6Al4V and SiAlON powders were prepared, weighed and blended in a T2F turbula mixer for 6 h in a dry medium, at a speed of 72 rpm. The admixture powders were loaded in a 250 ml cylindrical plastic vessel filled up to 10% level, and further placed in the mixing chamber and subjected to translational and rotational motions. The admixed powder was placed inside graphite die mould and pressed in an SPS machine type HHPD–25 (FCT Systeme GmbH, Germany). Sintering was carried out at the temperature of 1000–1100 °C for 10 and 30 min holding time, compaction pressure of 35 MPa and heating rate of 200 °C/min. During the sintering process, the temperature was monitored by an optical pyrometer focused on the surface of the graphite die. Four compositions of the composites were produced containing: Ti6Al4V alloy, 5, 10, 15 and 20 vol% SiAlON additions. The samples for tests carried out are densification, microstructural, hardness, phase analysis and fractography. The sintered densities were determined by the Archimedes principle. Density was determined by measuring the difference between the weight of the samples in air and then when it was suspended in distilled water. The relative density was calculated with reference to the theoretical density of the starting powders constituents using the rule of mixtures.

2.2 Microstructural and Phase Characterization of Sintered Composite

The microstructural analysis of the produced composites was characterized by optical microscopy, scanning electron microscopy and X-ray diffraction techniques. The sintered composites were prepared for metallography using grinding and polishing methods. The polished surfaces of the samples were etched by swab specimen up to 20 s using a solution containing 2 ml HCl, 6 ml Nitric acid and 92 ml distilled water, after which microstructural analysis was performed on the sintered composites. The ZEISS Axio observer optical microscope was used and complemented with TESCAN VEGA3 scanning electron microscopy equipped with energy dispersive spectroscopy (EDS). XRD analysis was done using a PANalytical Empyrean diffractometer (PW1710), with monochromatic Cu target Kα radiation at 40 kV and 40 mA. While the constituent phases of the sintered titanium composites were known using Highscore X'Pert Software.

2.3 Hardness and Fractography Analysis of the Composite

The hardness test was done for the produced composites by using a Vickers microhardness tester (FALCON 500 series) at room temperature on a polished parallel surface at a load of 100 gf (0.98 N) and dwell time of 15 s. The hardness indentation was repeated for a minimum of five times and an average hardness value was determined. While the fracture surfaces of the sintered titanium-based composite were observed using SEM to check the morphology pattern.

3 Results and Discussion

3.1 Effect of Sintering Parameters on Densification Mechanism

Figure 1a–c shows the effect of sintering temperature and displacement as a function of time for the sintered titanium-based composites. During the first 7 min period of the initial process at a temperature of 250 °C was kept and subsequently increased the sintering temperature to 1000 and 1100 °C individually and upheld for 10–30 min. Figure 1b at preliminary stage display an increase in displacement from 0.0 to 0.5 mm because of the effect of exerted pressure of 35 MPa even though the early temperature was too low to influence the material. The increase in temperature resulted in displacement and rearrangement of the powder particles as they compact together with the effect of pressure which becomes stronger and causes the escape of trapped air and

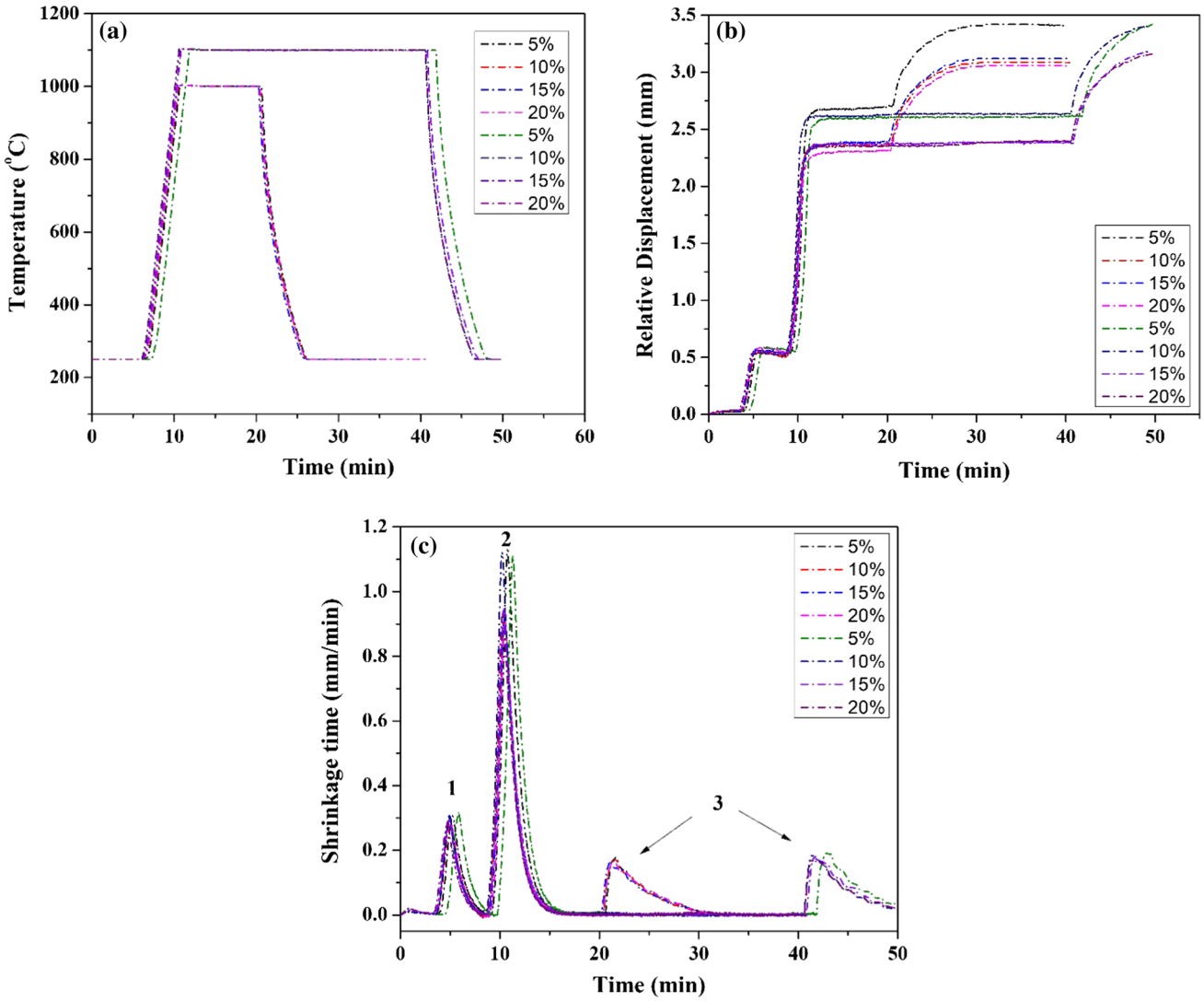

Fig. 1 Sintering parameters during SPS process against time: **a** sintering temperature, **b** relative displacement and **c** shrinkage rate

gas from the compact. The sintering processes goes together with neck growth due to the collective effects of evaporation and condensation which rises sintering temperature [19]. Increase in displacement indicates there was a transformation in the physical state and structure of the powders.

The mechanism of densification was explained utilizing the occurrences of shrinkage rate during SPS of the sintered composites. Figure 1c shows the shrinkage rate during spark plasma sintering of the total sintering time processes. A comparable trend of the sintering rate was displayed regardless of the sintering conditions which was categorized into three distinct shrinkage peaks. Stage 1 of the shrinkage rate is considered to have been involved with early rearrangement of mixed particle powders which is due to the relative motion of the various powders, gas removal and formation of spark existence between the titanium-based matrix and SiAlON particles because of applied pressure and drive occurring from the lower and upper punches [20]. Ghasali et al. [21] claimed that strengthening metal matrix with ceramic particles which are harder might cause an issue of gas removal during sintering and simply deform. Stage 2 of the shrinkage rate arose from 600 to 900 s is related to the effect of Joule heating of the localized plastic distortion at the interface of the particles. This stage during spark plasma sintering experiences powder surface-initiated from the titanium alloy and SiAlON particles because of high-pulse releases plasma made at powder contacts. Thus, an increase in temperature causes bonding taking place between the powder particles because of impacts at powder surfaces resulting in melting, arrangement and growth of the sintering necks at contact zone and movement of plastic flow [22]. At this stage, densification is developed and continue further through plastic distortion because of exerted pressure on them. Stage 3 signifies a greater deforming zone which

started after 1260 and 2400 s because of the holding time of 10 and 30 min respectively up until the sintering operation ends which was marks decrease in shrinkage rate. Due to the reduction in temperature and process of cooling of the spark plasma sintering compartment back to room temperature makes densification passage form accomplished [23, 24].

3.2 Effects of Spark Plasma Sintering on Relative Density

Figure 2 shows the effect of sintering temperature and time on the densification behavior of the sintered materials. Ti6Al4V with the addition of SiAlON ceramics sintered at 1000–1100 °C and 10–30 min holding time respectively which resulted in high densities of the sintered titanium-based composites ranging from 95 to 99%. It was noted that the relative density of the sintered composite decreased as the SiAlON content was increased from 5 to 20 vol%, as shown in Table 1. However, the decrease in relative density

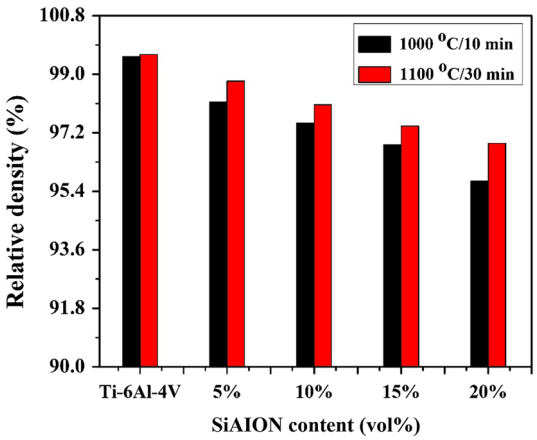

Fig. 2 Relative density of the SiAlON ceramic spark plasma sintered at different temperature and holding times

demonstrates that the composites contained a few porosities as the volume fraction of SiAlON particles increases. Thus, increasing the sintering temperature and holding time increased the relative density of the sintered composite ranging from 0.53 to 1.17% differences. This might be attributed to the positive effect of created plasma on the mobility and diffusion of atoms by vapouring and melting of powder particle surface during spark plasma sintering process [25]. This might also be identified with the initiation of grain development and the arrangement of structures with pores situated on the inside.

3.3 Microstructural and Phase Analysis of the Sintered Titanium-Based Composite

Figure 3a-b shows the optical micrograph of Ti6Al4V alloy which consists of two phases: lamellar alpha appears in the form of plates with light grey while beta phases were observed between alpha platelets with dark grey plates. This structure was in agreement with other reported structures where alpha phase has the highest volume fraction and the beta phase has a little volume fraction [26, 27]. Figures 3c–h and 4a–h shows typical microstructures of the SPS sintered composites with different content of ceramic reinforcing phase. The changes observed in the microstructure of sintered titanium matrix composites were associated with the sintering time and temperature. In all composites, the presence of pores was detected at the grain boundaries of sintered composites. The titanium matrix composite showed that the SiAlON particles were well dispersed in the matrix. Also, the increase in time and temperature of sintering revealed different sizes and morphologies of the microstructure. Falodun et al. [28] stated that advancement of titanium-based composite by adding particulates is anticipated to improve the grains, which are the direct result of the pinning effect on grain boundaries.

Table 1 The composition and sintering conditions, relative density, hardness values for spark sintered samples

Materials	Sintering conditions		Heating rate	Sintering pressure	Relative density	Hardness
	Temp (°C)	Time (min)	(°C/min)	(MPa)	(%)	($HV_{0.1}$)
Ti6Al4V	1000	10	200	35	99.54	363
	1100	30			99.61	396
Ti6Al4V + 5% SiAlON	1000	10	200	35	98.15	469
	1100	30			99.61	448
Ti6Al4V + 10% SiAlON	1000	10	200	35	97.50	497
	1100	30			98.06	453
Ti6Al4V + 15% SiAlON	1000	10	200	35	96.83	535
	1100	30			97.41	472
Ti6Al4V + 20% SiAlON	1000	10	200	35	95.71	574
	1100	30			96.88	561

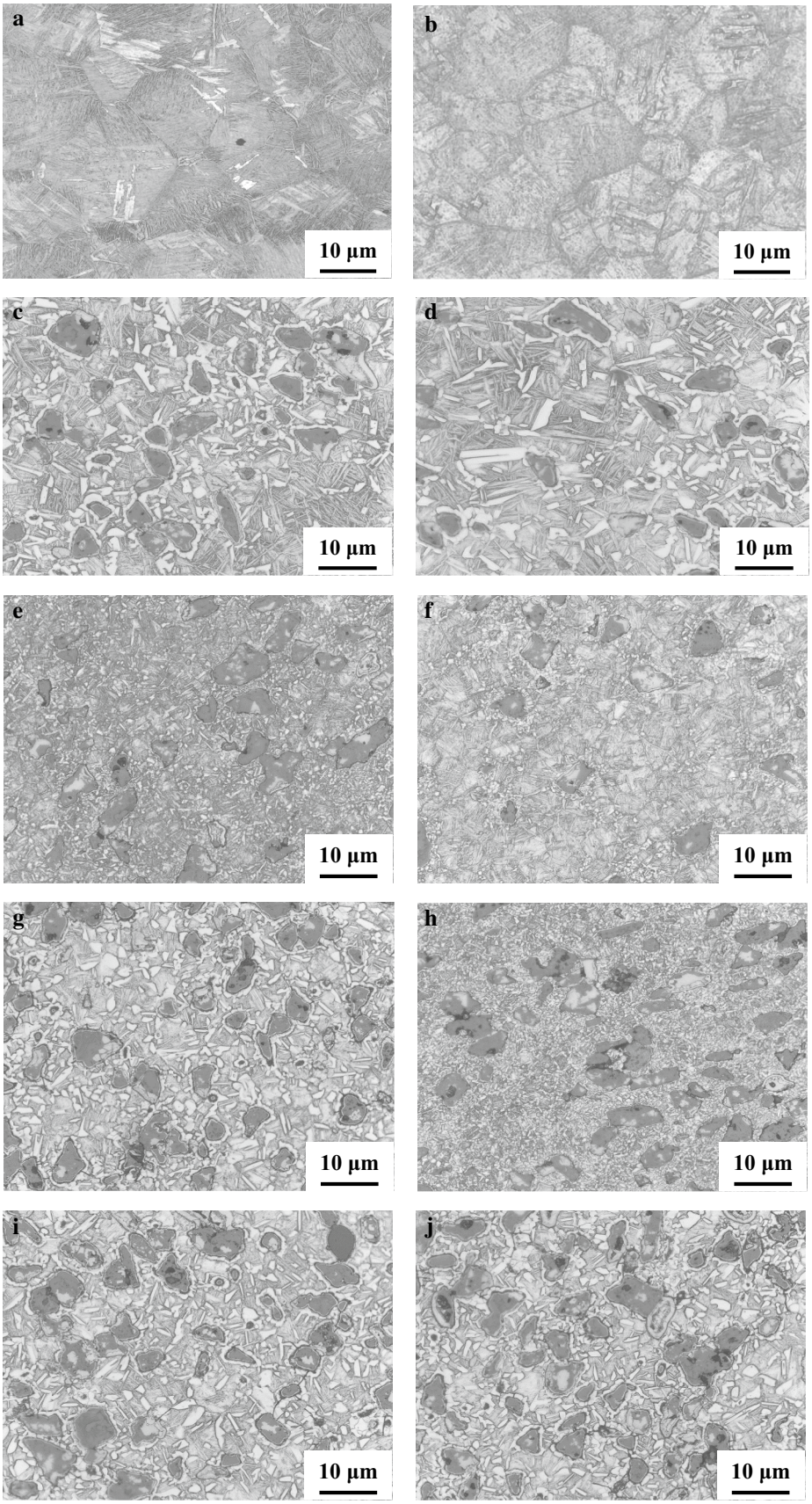

Fig. 3 Optical microstructure of sintered composites with different vol% SiAlON: left side represent the SPS parameters of 1000 °C/10 min, and the right hand represent 1100 °C/10 min holding time: **a**, **b** Ti6Al4V alloy; **c**, **d** 5%; **e**, **f** 10%; **g**, **h** 15% and **i**, **j** 20%

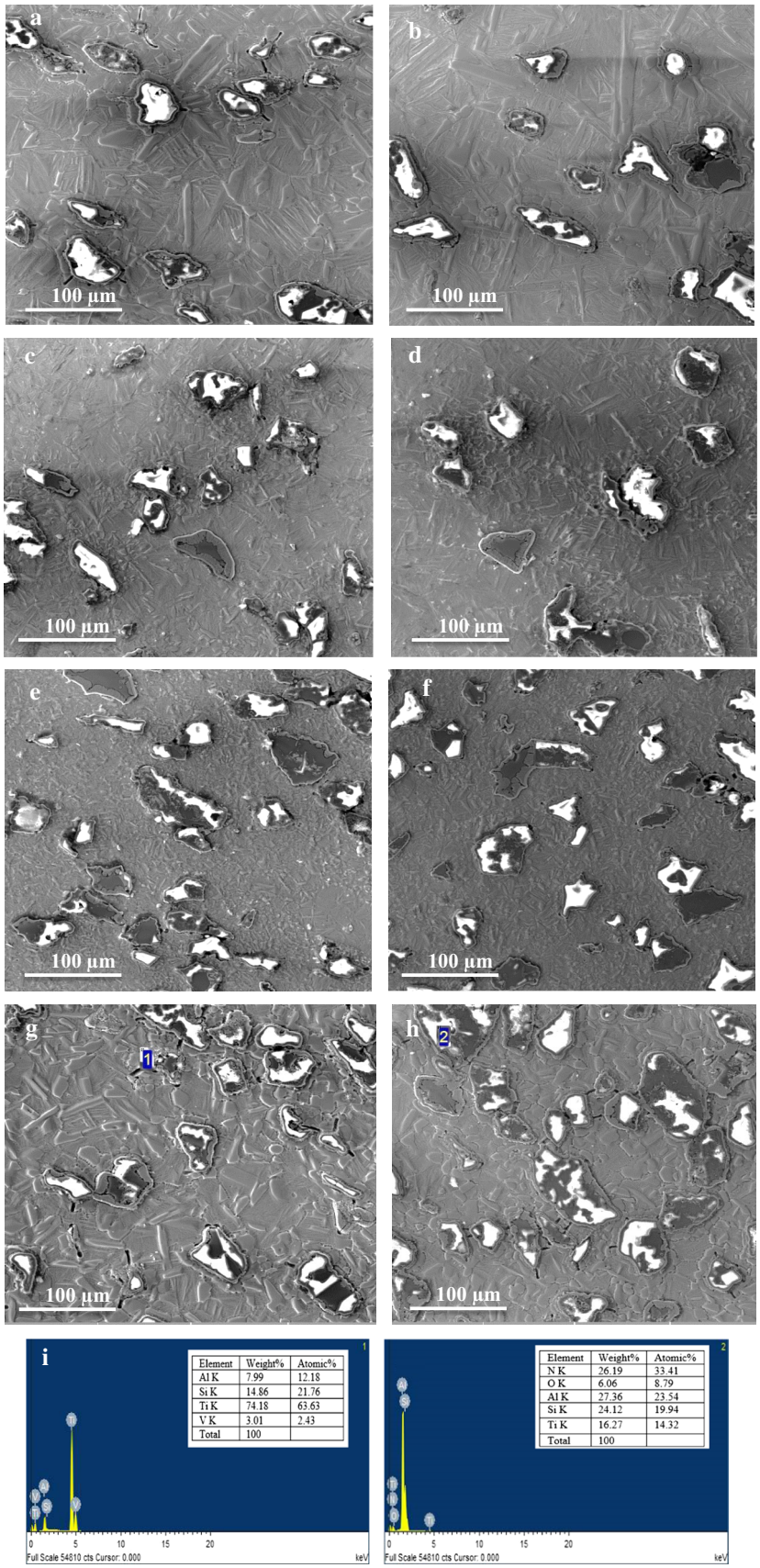

Fig. 4 SEM microstructure of sintered composites with different vol% SiAlON: left side represent the SPS parameters of 1000 °C/10 min, and the right hand represent 1100 °C/10 min holding time: **a**, **b** 5%; **c**, **d** 10%; **e**, **f** 15% and **g**, **h** 20%; and **i** EDS spectrum

The addition of SiAlON particle (20 vol%) in the matrix resulted in titanium matrix composite interfaces and further causes creation of some void sites which might be due to the weak bonding between Ti6Al4V alloy and SiAlON particle been observed in the Fig. 4. According to Koli et al. [29] and Sivakumar et al. [30] addition of more volume fraction of ceramic particle could lead to increase in porosity which might deteriorate the strength of the material because pores can nucleate at ceramic particle sites which further create an increase in contact surfaces which higher level of porosity. These porosities and formation of reaction region will bring inferior bonding interface between the matrix and reinforcement phases. Figure 4i shows the EDS spectrum, which is at the grain boundaries of the sintered titanium matrix composites, thus resulting in particulates reacting with the matrix.

The X-ray diffractogram of consolidated Ti6Al4V–SiAlON compacts at sintering temperature of 1000–1100 °C and the results of phase analysis are illustrated in Fig. 5. The SiO_2 which is noticed by XRD analysis as shown in all the sintered material and is thought to be formed due to the chemical reaction between Ti6Al4V with SiAlON. The patterns show distinct peak broadening and hereafter particle size and phases. It is observed that the height of the Ti peaks tends to decrease with increases in other forms of phases peak. The decrease in peaks height shows basic dislocation density as a result of imperfections that occurred owing to grain refinement of ceramic particles with titanium alloy.

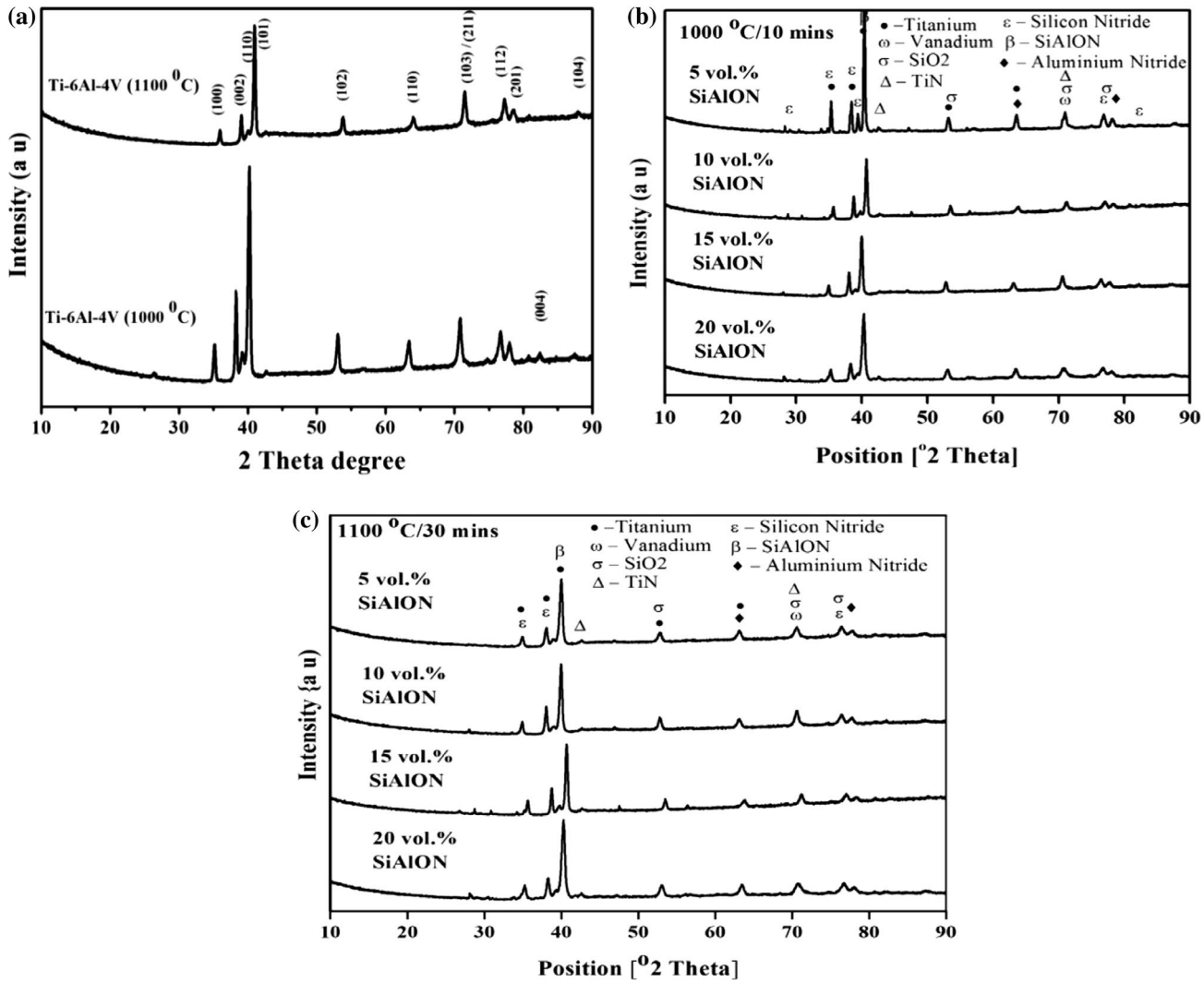

Fig. 5 X-ray diffraction pattern of **a** Ti6Al4V sintered at different temperatures, **b** sintered composite with 5–20 vol% SiAlON at 1000 °C and **c** 5–20 vol% SiAlON at 1100 °C

3.4 Effect of Sintering Parameters on Microhardness Values of Sintered Composites

The influence of sintering temperature and holding time on the microhardness of the sintered composites as presented in Fig. 6 and Table 1. Hardness was increased with respect to the sintering temperature and holding time with an increase in the varying volume fraction of reinforcement. The improve in hardness might be attributed to the presence of hard phases like Si_3N_4, TiN and SiO_2 within the matrix which makes obstruction for dislocation movement of the composite materials. However, phases formed might be due to an increase in sintering temperature and thus create an enhancement of thermal diffusion and further restrained dislocation movement. The increase in microhardness measurement display that the addition of 5–20 vol% SiAlON increases the hardness of the titanium matrix composite from 448 to 574 $HV_{0.1}$. The increase in microhardness can be described by the high hardness characteristics of the additional additives [31].

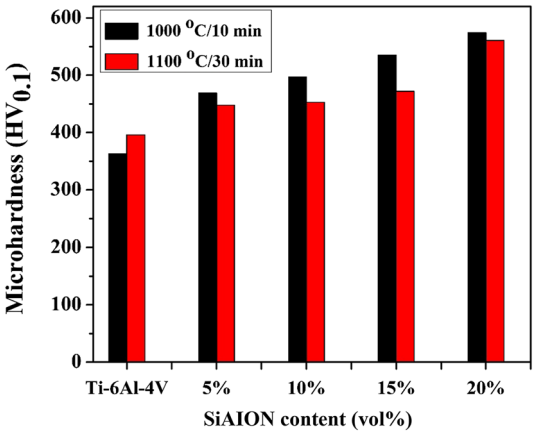

Fig. 6 Microhardness of Ti6Al4V alloy and Ti6Al4V with SiAlON composites

3.5 Fractography of the Sintered Titanium-Based Composite

Fracture surface SEM micrographs of the sintered titanium-based composite at different temperature and holding time are as shown in Figs. 7 and 8. The fracture morphology displays well-developed assistance among the particles as well as the changes in the fracture surfaces might be suggested due to

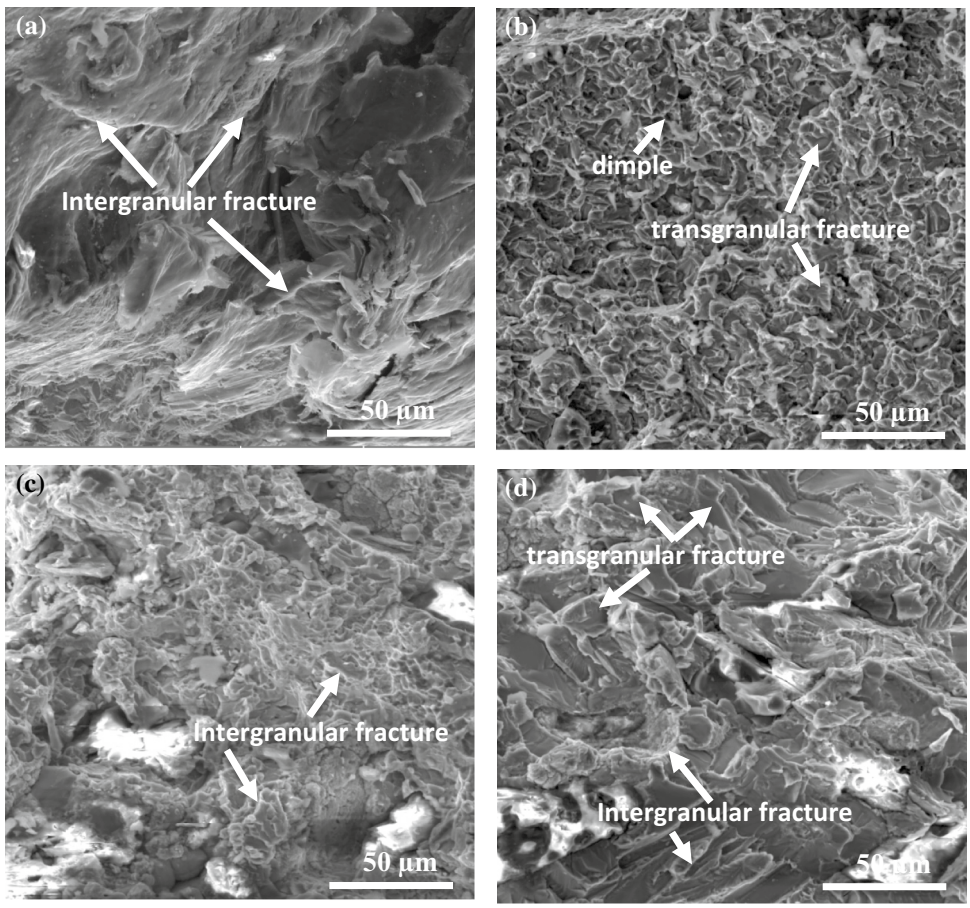

Fig. 7 SEM micrographs of fracture surfaces of sintered titanium matrix composites with SiAlON at 1000 °C/10 min **a** 5%, **b** 10%, **c** 15%, and **d** 20%

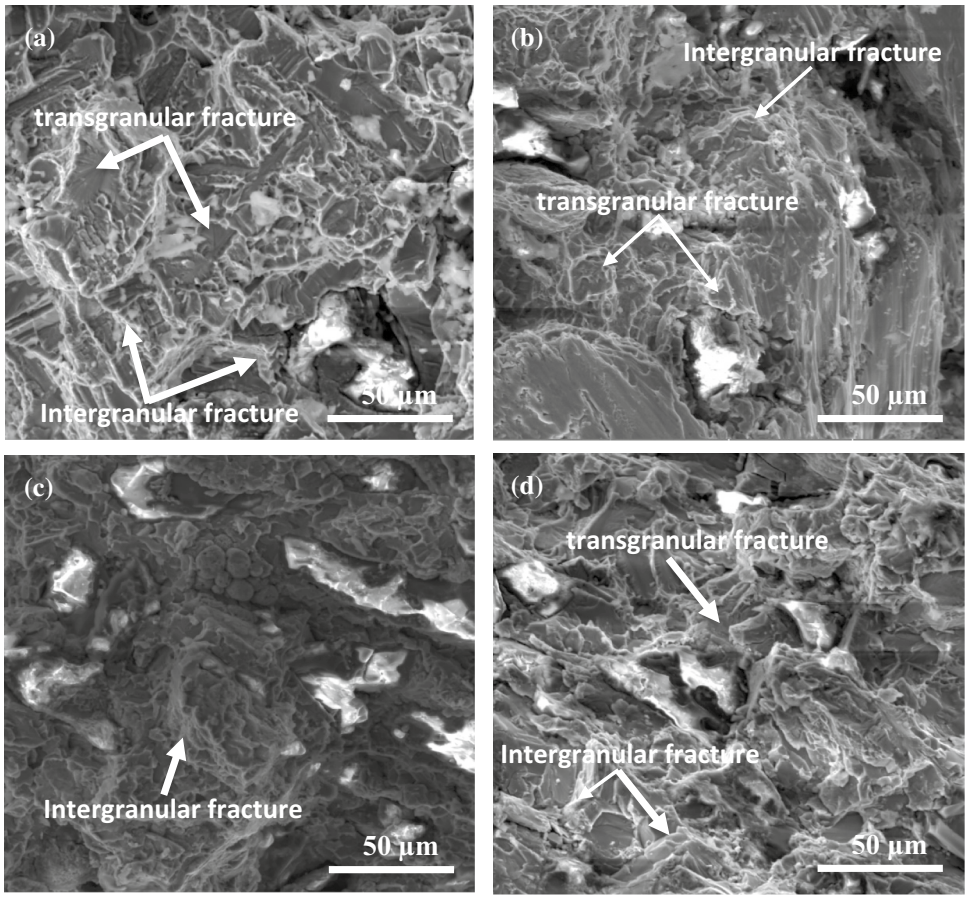

Fig. 8 SEM micrographs of fracture surfaces of sintered titanium matrix composites with SiAlON at 1100 °C/30 min **a** 5%, **b** 10%, **c** 15%, and **d** 20%

the increases in sintering temperature and holding time. Figures 7a–d and 8a–d show morphology of both intergranular and transgranular fracture with dimples features which could be attributed to the formation of different phases present in the titanium matrix composites. An intergranular crack features happen when the limits between the grains and the weakest districts in the material such as AlN and TiN. While transgranular cracks pass through from one grain to another grain as a result of diverse lattice direction in each grain. Nevertheless, with an increase in the volume fraction of SiAlON in the titanium matrix composite, dimples on the fracture surfaces were reduced with only dim traces left. This suggests that the fracture modes were a combination of ductile and brittle features. As can be seen from Figs. 7 and 8, the fracture modes do not cut across the reinforcement phase throughout the entire structure. Figures 7 and 8 shows a quasi-cleavage which is a brittle cleavage together with a ductile dimples [32].

4 Conclusion

The influence of the addition of SiAlON to reinforced titanium alloy composites fabricated by spark plasma sintering and the effect on densification mechanism, microstructural evolution, hardness and fractography was investigated. However, the following conclusions were drawn from the discussions;

1. A uniform distribution of SiAlON particles in the titanium matrix was revealed.
2. The addition of SiAlON reinforcements to the titanium matrix significantly increases the microhardness, while the density slightly decreases upon addition of the ceramic.
3. The effect of sintering temperature and time made known with changes in the microstructure and formation with the growth of new phases in the titanium-based composites. Also, the increasing in time and temperature of sintering revealed different sizes and morphologies of the microstructure.
4. The fracture morphology of the sintered TMCs showed both intergranular and transgranular transformation within the matrix with fine dimples features. Also, the fractography behavior additional changed from multiple arrangements to a predominantly transgranular one.

Acknowledgements The authors would like to acknowledge the Global Excellence and Stature at the University of Johannesburg and National Research Foundation, South Africa for providing the necessary financial supports. Also, the Institute of Nanoengineering Research at the Tshwane University of Technology in using spark plasma sintering facility.

References

1. O.E. Falodun, B.A. Obadele, S.R. Oke, O.O. Ige, P.A. Olubambi, M.L. Lethabane, S.W. Bhero, Influence of spark plasma sintering on microstructure and wear behaviour of Ti–6Al–4V reinforced with nanosized TiN. Trans. Nonferr. Metals Soc. China **28**, 47–54 (2018)
2. K. Kondoh, T. Threrujirapapong, J. Umeda, B. Fugetsu, High-temperature properties of extruded titanium composites fabricated from carbon nanotubes coated titanium powder by spark plasma sintering and hot extrusion. Compos. Sci. Technol. **72**, 1291–1297 (2012)
3. L. Yan, W.-J. Guo, L. Ying, Bimodal-grained Ti fabricated by high-energy ball milling and spark plasma sintering. Trans. Nonferr. Metals Soc. China **26**, 1170–1175 (2016)
4. F. Weng, C. Chen, H. Yu, Research status of laser cladding on titanium and its alloys: a review. Mater. Des. **58**, 412–425 (2014)
5. S.C. Tjong, Y.-W. Mai, Processing-structure-property aspects of particulate-and whisker-reinforced titanium matrix composites. Compos. Sci. Technol. **68**, 583–601 (2008)
6. H. Tsang, C. Chao, C. Ma, Effects of volume fraction of reinforcement on tensile and creep properties of in situ TiB/Ti MMC. Scripta Mater. **37**, 1359–1365 (1997)
7. B.A. Obadele, O.E. Falodun, S.R. Oke, P.A. Olubambi, Spark plasma sintering behaviour of commercially pure titanium micro-alloyed with Ta–Ru. Part. Sci. Technol. **37**, 886–892 (2019)
8. O.E. Falodun, B.A. Obadele, S.R. Oke, M.E. Maja, P.A. Olubambi, Effect of sintering parameters on densification and microstructural evolution of nano-sized titanium nitride reinforced titanium alloys. J. Alloys Compd. **736**, 202–210 (2018)
9. Z.-H. Zhang, X.-B. Shen, F.-C. Wang, W. Sai, S.-K. Li, H.-N. Cai, Microstructure characteristics and mechanical properties of TiB/Ti-1.5 Fe-2.25 Mo composites synthesized in situ using SPS process. Trans. Nonferr. Metals Soc. China **23**, 2598–2604 (2013)
10. S. Maseko, O. Fayomi, Characterization of ceramic reinforced titanium matrix composites fabricated by spark plasma sintering for anti-ballistic applications. Def. Technol. **14**, 408–411 (2018)
11. T. Ekström, M. Nygren, SiAlON ceramics. J. Am. Ceram. Soc. **75**, 259–276 (1992)
12. F.L. Riley, Silicon nitride and related materials. J. Am. Ceram. Soc. **83**, 245–265 (2000)
13. B. Basu, J. Vleugels, M. Kalin, O. Van Der Biest, Friction and wear behaviour of SiAlON ceramics under fretting contacts. Mater. Sci. Eng., A **359**, 228–236 (2003)
14. N.C. Acikbas, S. Tegmen, S. Ozcan, G. Acikbas, Thermal shock behaviour of α: β-SiAlON–TiN composites. Ceram. Int. **40**, 3611–3618 (2014)
15. O.E. Falodun, B.A. Obadele, S.R. Oke, O.O. Ige, P.A. Olubambi, Effect of TiN and TiCN additions on spark plasma sintered Ti–6Al–4V, Part. Sci. Technol. (2018). https://doi.org/10.1080/02726351.2018.1515798
16. R. Sivakumar, K. Aoyagi, T. Akiyama, Thermal conductivity of combustion synthesized β-sialons. Ceram. Int. **35**, 1391–1395 (2009)
17. M.E. Maja, O.E. Falodun, B.A. Obadele, S.R. Oke, P.A. Olubambi, Nanoindentation studies on TiN nanoceramic reinforced Ti–6Al–4V matrix composite. Ceram. Int. **44**, 4419–4425 (2018)
18. G. Cao, R. Metselaar, alpha.'-Sialon ceramics: a review. Chem. Mater. **3**, 242–252 (1991)
19. Z. Zhang, X. Shen, F. Wang, S. Lee, L. Wang, Densification behavior and mechanical properties of the spark plasma sintered monolithic TiB2 ceramics. Mater. Sci. Eng., A **527**, 5947–5951 (2010)
20. S. Oke, O. Ige, O. Falodun, M.R. Mphahlele, P. Olubambi, Densification behavior of spark plasma sintered duplex stainless steel reinforced with TiN nanoparticles, in: *IOP Conference Series: Materials Science and Engineering*, IOP Publishing, 2018, p. 012034
21. E. Ghasali, K. Shirvanimoghaddam, A.H. Pakseresht, M. Alizadeh, T. Ebadzadeh, Evaluation of microstructure and mechanical properties of Al–TaC composites prepared by spark plasma sintering process. J. Alloys Compd. **705**, 283–289 (2017)
22. S.R. Oke, O.O. Ige, O.E. Falodun, A.M. Okoro, M.R. Mphahlele, P.A. Olubambi, Powder metallurgy of stainless steels and composites: a review of mechanical alloying and spark plasma sintering. Int. J. Adv. Manuf. Technol. **102**, 3271–3290 (2019)
23. Y. Cheng, Z. Cui, L. Cheng, D. Gong, W. Wang, Effect of particle size on densification of pure magnesium during spark plasma sintering. Adv. Powder Technol. **28**, 1129–1135 (2017)
24. S. Diouf, A. Molinari, Densification mechanisms in spark plasma sintering: effect of particle size and pressure. Powder Technol. **221**, 220–227 (2012)
25. Y. Song, Y. Li, Z. Zhou, Y. Lai, Y. Ye, A multi-field coupled FEM model for one-step-forming process of spark plasma sintering considering local densification of powder material. J. Mater. Sci. **46**, 5645–5656 (2011)
26. A. Taşdemirci, A. Hızal, M. Altındiş, I.W. Hall, M. Güden, The effect of strain rate on the compressive deformation behavior of a sintered Ti6Al4V powder compact. Mater. Sci. Eng., A **474**, 335–341 (2008)
27. M.T. Jovanović, S. Tadić, S. Zec, Z. Mišković, I. Bobić, The effect of annealing temperatures and cooling rates on microstructure and mechanical properties of investment cast Ti–6Al–4V alloy. Mater. Des. **27**, 192–199 (2006)
28. O.E. Falodun, B.A. Obadele, S.R. Oke, A.M. Okoro, P.A. Olubambi, Titanium-based matrix composites reinforced with particulate, microstructure, and mechanical properties using spark plasma sintering technique: a review. Int. J. Adv. Manuf. Technol. **102**, 1689–1701 (2019)
29. G. Sivakumar, V. Ananthi, S. Ramanathan, Production and mechanical properties of nano SiC particle reinforced Ti–6Al–4V matrix composite. Trans. Nonferr. Metals Soc. China **27**, 82–90 (2017)
30. D.K. Koli, G. Agnihotri, R. Purohit, Properties and characterization of Al-Al_2O_3 composites processed by casting and powder metallurgy routes. Int. J. Latest Trends Eng. Technol. **2**, 486–496 (2013)
31. O. Falodun, B. Obadele, S. Oke, M. Maja, P. Olubambi, Synthesis of Ti–6Al–4V alloy with nano-TiN microstructure via spark plasma sintering technique, in: *IOP conference series: Materials science and engineering*, IOP Publishing, 2017, p. 012029
32. R. Naik, W. Pollock, W. Johnson, Effect of a high-temperature cycle on the mechanical properties of silicon carbide/titanium metal matrix composites. J. Mater. Sci. **26**, 2913–2920 (1991)